Ab Initio Study of Superalkalis. First Ionization Potentials and Thermodynamic Stability

Eva Rehm, Alexander I. Boldyrev,[†] and Paul von R. Schleyer*

Institut für Organische Chemie, Friedrich-Alexander Universität Erlangen-Nürnberg, Henkestrasse 42,
8520 Erlangen, Germany

Received January 31, 1992

The equilibrium geometries and fundamental frequencies of the Li_2F^+, Li_2F, Na_2Cl^+, Na_2Cl, Li_2O, Li_3O^+, Li_3O, Li_2S, Li_3S^+, Li_3S, Na_2O, Na_3O^+, Na_3O, Li_3N, Li_4N^+, Li_4N, Li_3P, Li_4P^+, and Li_4P species were calculated at MP2-FULL/6-31+G*. The total energies at these geometries were calculated at the MP4SDTQ and QCISD(T) levels with the 6-31+G*, 6-311+G*, and 6-311+G(2df) basis sets. The global minima are as follows: linear Li_2F^+, Na_2Cl^+, Na_2O ($D_{\infty h}$, $^1\Sigma^+$); angular Li_2O, Li_2S (C_{2v}, $^1A_1$) and Li_2F, Na_2Cl (C_{2v}, $^2A_1$); planar Li_3O^+, Li_3S^+, Na_3O^+, Li_3N (D_{3h}, $^1A_1'$) and Li_3O, Na_3O (D_{3h}, $^2A_1'$); pyramidal Li_3P (C_{3v}, $^1A_1$) and Li_3S (C_{3v}, $^2A_1$); tetrahedral Li_4N^+, Li_4P^+ (T_d, $^1A_1$) and Li_4N (T_d, $^2A_1$); distorted tetrahedral Li_4P (C_{2v}, $^2A_1$). All cationic and neutral species are stable toward loss of alkali metal cation M^+ or alkali metal atom M, respectively. All Li_2F, Na_2Cl, Li_3O, Li_3S, Na_3O, Li_4N, and Li_4P species possess lower first ionization potentials (FIP) than the Cs atom (3.9 eV) and therefore are termed "superalkalis".

Introduction

Among all chemical elements the alkali metals possess the lowest ionization potentials (IP (in eV)): Li, 5.39; Na, 5.14; K, 4.34; Rb, 4.17; Cs, 3.89.[1] However, in the last 15 years many stable molecules with even lower IPs have been identified. These alkali metal clusters[2,3] and hyperalkali molecules ML_{k+n} (where L is an alkali metal atom, k the normal valency of the central atom M, and $n \geq 1$)[4,5] may be considered to be "superalkaline".[5b,f] Among the small alkali metal clusters, triatomic combinations have the lowest IPs (e.g. Li_2 = 4.86, Li_3 = 4.35, Li_4 = 4.69, Li_5 = 4.56, and Li_6 = 4.67 eV[2i]). Similarly, hyperalkali molecules ML_{k+n} with n = 1 have the lowest IPs (e.g. NaO = 6.5, Na_2O = 5.06, Na_3O = 3.90, and Na_4O = 3.95 eV[4c]). Such superalkali molecules may serve as components of new nontraditional salts, for instance $ML_{k+1}^+X^-$ with ML_{k+1}^+ cations (e.g. Li_3O^+, Li_4N^+, etc.). Moreover, the low IP of ML_{k+1} species may allow the synthesis of new salts $ML_{k+1}^+X^-$ in which corresponding neutral atoms or molecules X possess low electron affinities (AE).

The IPs of Li_2F, Li_2Cl, Na_2F, Na_2Cl, Cs_2F, Cs_2Cl, Li_3O, Li_3S, Na_3O, Na_3S, Li_4N, Li_4P, Na_4N, and Na_4P were investigated theoretically by the discrete-variational-$X\alpha$ (DV-$X\alpha$) method using the Slater-transition approximation (IPs were computed with $n_{HOMO} = 1/2$).[5b,f] These calculations were carried out at the equilibrium geometries of the corresponding cations, and the IPs of the ML_{k+1} radicals were assumed to be equal to the vertical EA values of the ML_{k+1}^+ cations. All calculated IPs were found to be 3.7 eV or lower and thus less than the IPs of alkali metal atoms. However, due to the limitations in the DV-$X\alpha$ theory, the calculated IPs were usually lower than available experimental data: Na_2Cl, 3.7 eV (calcd[5b]) vs 4.15 eV (exptl[4b]); Li_3O, 3.4 eV (calcd[5b]) vs 4.45 eV (exptl[4a]); Na_3O, 3.5 eV (calcd[5b]) vs 3.98 eV (exptl[4c]); Li_3S, 3.2 eV (calcd[5b]) vs 6.65 eV (exptl[6]). Large discrepancies are found with Li_3O and Li_3S. We have now refined the calculations of the IPs of several superalkali species at high ab initio levels using equilibrium geometries both for neutral and for cation forms. We have computed the dissociation energies and the vibrational frequencies of these species, as well.

Computational Methods

The geometries of LiF, Li_2F^+, Li_2F, NaCl, Na_2Cl^+, Na_2Cl, Li_2O, Li_3O^+, Li_3O, Li_2S, Li_3S^+, Li_3S, Na_2O, Na_3O^+, Na_3O, Li_3N, Li_4N^+, Li_4N, Li_3P, Li_4P^+, and Li_4P were optimized employing analytical gradients[7] with a polarized split-valence basis set augmented with diffuse functions

† Permanent address: Institute of Chemical Physics, Russian Academy of Sciences, Kosygin Str. 4, Moscow v-334, Russia.

(1) Lias, S. G.; Bartmess, J. E.; Liebman, J. F.; Holmes, J. L.; Levin, R. D.; Mallard, W. G. *Gas-Phase Ion and Neutral Thermochemistry. J. Phys. Chem. Ref. Data, Supp. 1* **1988**, 17.

(2) (a) Hart, A.; Goodfried, P. L. *J. Chem. Phys.* **1975**, *62*, 1306. (b) Wu, C. H. *J. Chem. Phys.* **1976**, *65*, 3181. (c) Herrmann, A.; Schumacher, E.; Wöste, L. *J. Chem. Phys.* **1978**, *68*, 2327. (d) Kappes, M. M.; Kunz, R. W.; Schumacher, E. *Chem. Phys. Lett.* **1982**, *91*, 413. (e) Peterson, K. I.; Dao, P. D.; Farley, R. W.; Castleman, A. W., Jr. *J. Chem. Phys.* **1984**, *80*, 1780. (f) Brechignac, C.; Cahuzac, Ph. *Chem. Phys. Lett.* **1985**, *117*, 365. (g) Broyer, M.; Cheveleyre, J.; Delacretaz, D.; Fayet, P.; Wöste, L. *Chem. Phys. Lett.* **1985**, *114*, 477. (h) Saunders, W. A.; Clemenger, K.; de Heer, W. A.; Knight, W. D. *Phys. Rev.* **1985**, *B32*, 1366. (i) Brechignac, C.; Cahuzac, Ph.; Roux, J. Ph. *Chem. Phys. Lett.* **1986**, *127*, 445. (j) Wu, C. H. *J. Chem. Phys.* **1989**, *91*, 546.

(3) (a) Chou, M. Y.; Cleland, A.; Cohen, M. L. *Solid State Commun.* **1984**, *52*, 645. (b) Chou, M. Y.; Cohen, M. L. *Phys. Lett.* **1986**, *113A*, 420. (c) Ishii, Y.; Ohnishi, S.; Sugano, S. *Phys. Rev.* **1986**, *33B*, 5271. (d) Koutecky, J.; Fantucci, P. *Chem. Rev.* **1986**, *86*, 539. (e) Knight, W. D.; De Heer, W. A.; Sauders, W. A.; Clemenger, K.; Chou, M. Y.; Cohen, M. L. *Chem. Phys. Lett.* **1987**, *134*, 1. (f) Boustani, I.; Pewestorf, W.; Fantucci, P.; Bonacic-Koutecky, V.; Koutecky, J. *Phys. Rev.* **1987**, *35B*, 9437. (g) Bonacic-Koutecky, V.; Boustani, I.; Guest, M.; Koutecky, J. *J. Chem. Phys.* **1988**, *89*, 4861. (h) Spiegelmann, F.; Pavolini, D. *J. Chem. Phys.* **1988**, *89*, 4954. (i) Bonacic-Koutecky, V.; Fantucci, P.; Koutecky, J. *Phys. Rev.* **1988**, *37B*, 4369.

(4) (a) Wu, C. H.; Kudo, H.; Ihle, H. R. *J. Chem. Phys.* **1979**, *70*, 1815. (b) Peterson, K. I.; Dao, P. D.; Castleman, A. W., Jr. *J. Chem. Phys.* **1983**, *79*, 777. (c) Dao, P. D.; Peterson, K. I.; Castleman, A. W., Jr. *J. Chem. Phys.* **1984**, *80*, 563. (d) Wu, C. H. *Chem. Phys. Lett.* **1987**, *139*, 357. (e) Kuan, T.-C.; Jiang, R.-C.; Su, T.-M. *J. Chem. Phys.* **1990**, *92*, 2553. (f) Kudo, H.; Wu, C. H. *Chem. Express* **1990**, *5*, 633. (g) Pollack, S.; Wang, C. R. C.; Kapes, M. M. *Chem. Phys. Lett.* **1990**, *175*, 209. (h) Kudo, H.; Zmbov, K. F. *Chem. Phys. Lett.* **1991**, *187*, 77.

(5) (a) Schleyer, P. v. R.; Würthwein, E.-U.; Pople, J. A. *J. Am. Chem. Soc.* **1982**, *104*, 5839. (b) Gutsev, G. L.; Boldyrev, A. I. *Chem. Phys. Lett.* **1982**, *92*, 262. (c) Schleyer, P. v. R. In *New Horizons of Quantum Chemistry*; Lowdin, P.-O., Pullman, B., Eds.; Reidel: Dordrecht, The Netherlands, 1983; pp 95–105. (d) Schleyer, P. v. R.; Würthwein, E.-U.; Kaufmann, E.; Clark, T. *J. Am. Chem. Soc.* **1983**, *105*, 5930. (e) Schleyer, P. v. R.; Tidor, B.; Jemmis, E. D.; Chandrasekhar, J.; Würthwein, E.-U.; Kos, A. J.; Luke, B. T.; Pople, J. A. *J. Am. Chem. Soc.* **1983**, *105*, 484. (f) Gutsev, G. L.; Boldyrev, A. I. *Adv. Chem. Phys.* **1985**, *51*, 169. (g) Klimenko, N. M.; Musaev, D. G.; Gorbik, A. A.; Zyubin, A. S.; Charkin, O. P.; Würthwein, E.-U.; Schleyer, P. v. R. *Koord. Khim.* **1986**, *12*, 601. (h) Pewerstorf, V.; Koutecky, J. *J. Chem. Phys.* **1988**, *89*, 5794. (i) Fantucci, P.; Bonacic-Koutecky, V.; Pewestorf, W.; Koutecky, J. *J. Chem. Phys.* **1989**, *91*, 4229. (j) Mebel, A. M.; Klimenko, N. M.; Charkin, O. P. *Zh. Strukt. Khim.* **1988**, *29*, N3, 12. (k) Klimenko, N. M.; Mebel, A. M.; Charkin, O. P. *Zh. Strukt. Khim.* **1988**, *29*, N3, 22. (l) Würthwein, E.-U.; Sen, K. D.; Pople, J. A.; Schleyer, P. v. S. *Inorg. Chem.* **1983**, *22*, 496. (m) Würthwein, E.-U.; Schleyer, P. v. R.; Pople, J. A. *J. Am. Chem. Soc.* **1984**, *106*, 6973.

(6) Wu, C. H.; Kudo, H. Private communications.

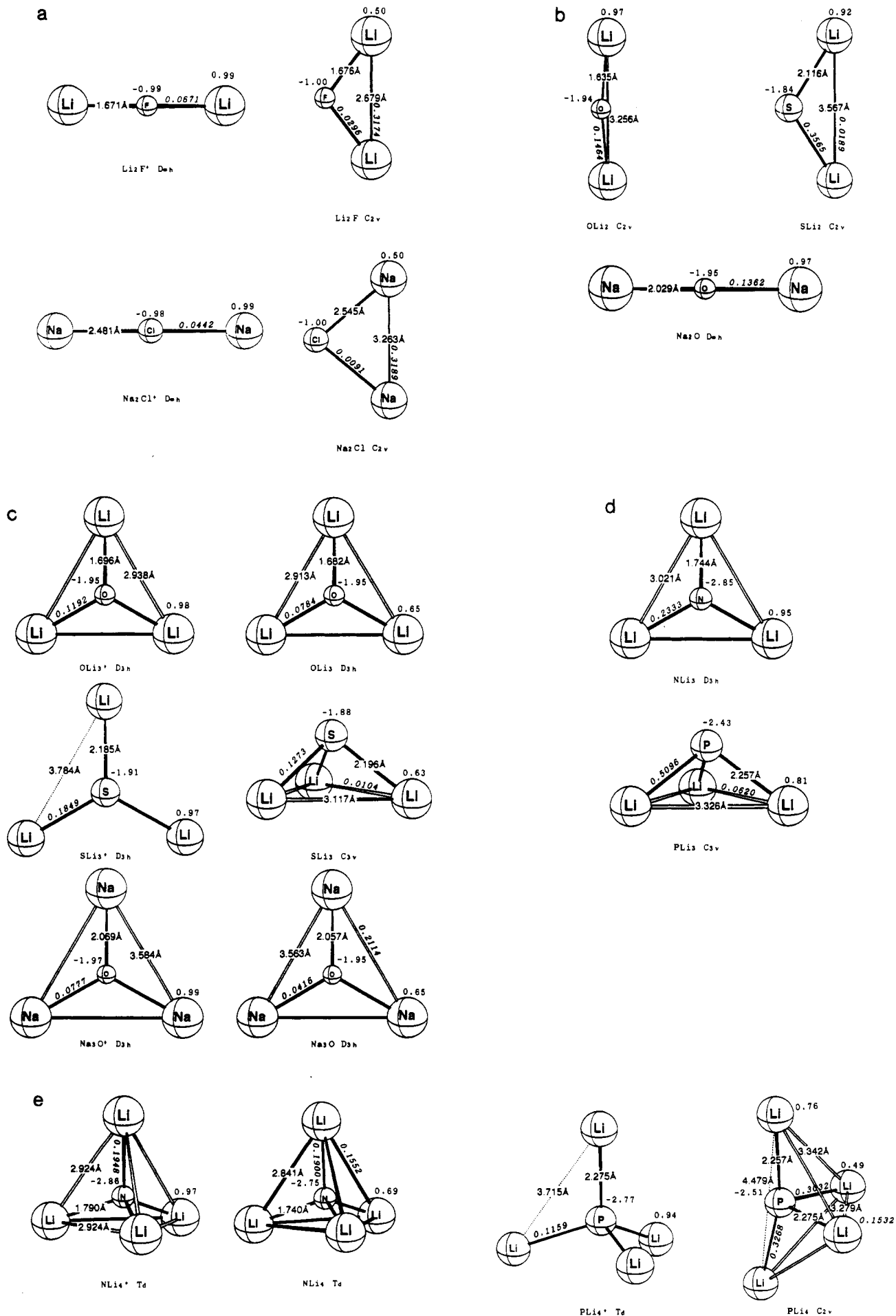(7) Schlegel, H. B. *J. Comput. Chem.* **1982**, *3*, 214.

Figure 1. Geometries of superalkali compounds with bond lengths (Å), natural charges (e), and overlap weighted NAO bond orders.[33,34]
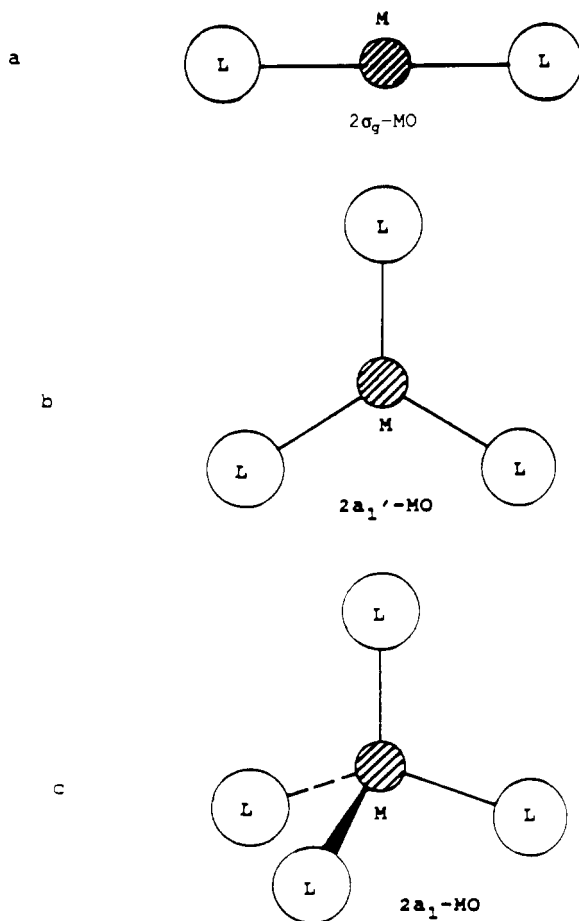
Figure 2. Highest occupied molecular orbitals (HOMOs) of superalkali compounds.

(HF/6-31+G*)[8-10] and at correlated (MP2-FULL/6-31+G*) levels (UHF and UMP2-FULL for open shell systems). Parts a–e of Figure 1 display the geometries. Fundamental frequencies, normal coordinates, and zero point energies (ZPE) were calculated by using standard FG matrix methods.[10] The MP2-FULL/6-31+G* equilibrium geometries were used to evaluate electron correlation corrections in the frozen-core approximation both by Moller–Plesset perturbation theory to full fourth order[11] and by the (U)QCISD(T)[12] method using the 6-311+G* and the 6-311+G(2df) basis sets. The UHF wave functions for open shell systems were projected to pure spectroscopic states (PUHF, PMP2, PMP3, and PMP4).[13] Analytical frequencies at MP2-FULL/6-31+G* for closed shell systems were carried out with the CADPAC program,[14] while GAUSSIAN 90 (CONVEX version)[15]was used for the other calculations. The total energies at different correlated levels are presented in Table I. Dissociation energies and ionization potentials are given in Tables II and III, respectively. The first harmonic frequencies are summarized in Table IV.

Results and Discussion

Li$_2$F$^+$, Li$_2$F, Na$_2$Cl$^+$, and Na$_2$Cl. Experimental geometries and frequencies of Li$_2$F$^+$ and Na$_2$Cl$^+$ are not known, but the

(8) Hariharan, P. C.; Pople, J. A. *Theor. Chim. Acta* **1973**, *28*, 213.

(9) (a) Clark, T.; Chandrasekhar, J.; Spitznagel, G.-W.; Schleyer, P. v. R. *J. Comput. Chem.* **1983**, *4*, 294. (b) Frisch, M. J.; Pople, J. A.; Binkley, J. S. *J. Chem. Phys.* **1984**, *80*, 3265.

(10) Hehre, W. J.; Radom, L.; Schleyer, P. v. R.; Pople, J. A. *Ab Initio Molecular Orbital Theory*; Wiley: New York, 1986.

(11) Raghavachari, K.; Pople, J. A. *Int. J. Quant. Chem.* **1978**, *12*, 91.

(12) Pople, J. A.; Head-Gordon, M.; Raghavachari, K. *J. Chem. Phys.* **1987**, *87*, 5968.

(13) Schlegel, H. B. *J. Chem. Phys.* **1986**, *84*, 4530.

(14) CADPAC. Amos, R. D.; Rice, J. E. CADPAC: The Cambridge Analytic Derivatives Package, issue 4.0. Cambridge, 1987.

(15) GAUSSIAN 90 (convex version). Frisch, M. J.; Head-Gordon, M.; Trucks, G. W.; Foresman, J. B.; Schlegel, H. B.; Raghavachari, K.; Robb, M. A.; Binkley, J. S.; Gonzales, C.; DeFrees, D. J.; Fox, D. J.; Whiteside, R. A.; Seeger, R.; Melius, C. F.; Baker, J.; Martin, R.; Kahn, L. R.; Stewart, J. J. P.; Fluder, E. M.; Topiol, S.; Pople, J. A. Gaussian Inc., Pittsburgh, PA, 1990.

experimental heat of formation of Na$_2$Cl$^+$ and its dissociation energy into NaCl + Na$^+$ (D_0 = 41.3 kcal/mol) are available.[16] According to published ab initio data (only at the HF level) the Li$_2$F$^+$ cation is linear ($D_{\infty h}$ symmetry), L$^+$–Hal$^-$–L$^+$, with R_e-(Li–F) = 1.68 Å[5c,17] (longer than in LiF, R_e(Li–F) = 1.563 864 Å[18]). We optimized Li$_2$F$^+$ and Na$_2$Cl$^+$ at the correlated MP2-(FULL)/6-31+G* level. Both species are linear (no imaginary frequencies) with bond lengths 1.671 Å for Li$_2$F$^+$ and 2.481 Å for Na$_2$Cl$^+$ (see Figure 1a). At our highest level (QCISD(T)/6-311+G(2df)//MP2(FULL)/6-31+G*+ZPE) the dissociation energies, Li$_2$F$^+$ → LiF + Li$^+$ and Na$_2$Cl$^+$ → NaCl + Na$^+$, are 67.9 and 48.0 kcal/mol, respectively.

The extra electrons in the neutral linear species Li$_2$F and Na$_2$-Cl ($D_{\infty h}$ symmetry) occupy 2σ-MOs (see Figure 2). Although those MOs are antibonding with respect to the central atom–ligand interaction, their energy should be lower than the 2s(3s)-AO energy of the isolated Li (Na) atom.[5b] The earlier DVM-X$_\alpha$ calculations for linear Li$_2$F and Na$_2$Cl (at cation geometry) agree with this qualitative picture:[5b] the IPs of Li$_2$F and Na$_2$Cl (3.7 eV) are lower than the IPs of Li (5.39 eV)[1] and of Na (5.14 eV).[37] However, the neutral compounds Li$_2$F and Na$_2$Cl are not stable toward angular deformation, because the 2σ-MOs in these species are ligand–ligand bonding. Accordingly, these neutral species deform to give shorter L···L distances and better ligand AO overlap. The previous Hartree–Fock calculations of Na$_2$Cl led to a C_{2v} equilibrium geometry with a Na–Cl–Na bond angle of 78.9°, a Na–Cl bond length of 2.566 Å, and a Na···Na distance of 3.261 Å.[19] A corresponding C_{2v} structure with a linearization barrier of only 2.6 kcal/mol had been found for Li$_2$F (R(F–Li) = 1.617 Å, ∠Li–F–Li = 117.9°).[5c] The resulting geometric and electronic structure is well described as Na$_2$$^{•+}Cl^-$ [19,20]—and the same is true for Li$_2$$^{•+}F^-$. The experimental dissociation energy of Na$_2$Cl → NaCl + Na was estimated to be 18.0 kcal/mol[21] and a IP of 4.15 ± 0.2 eV was found.[4b]

Optimization of both Li$_2$F and Na$_2$Cl at UMP2-FULL/6-31+G* led to angular C_{2v} structures (^{2}A$_1$ state) with R(Li–F) = 1.676 Å, R(Li···Li) = 2.696 Å, and ∠Li–F–Li = 107.1° and R(Na–Cl) = 2.545 Å, R(Na···Na) = 3.263 Å, and ∠Na–Cl–Na = 79.7°, respectively (Figure 1a). Both neutral species are minima (no imaginary frequencies). The calculated Li···Li and Na···Na distances are intermediate between bond lengths in neutral Li$_2$ (2.777 Å) and Na$_2$ (3.153 Å), on the one hand, and the charged Li$_2$$^{•+}$ (3.160 Å) and Na$_2$$^{•+}$ (3.653 Å) radical cations (all geometries optimized at MP2-FULL/6-31+G*), on the other. The calculated dissociation energies of Li$_2$F → LiF + Li and Na$_2$Cl → NaCl + Na are 33.1 and 20.1 kcal/mol (QCISD(T)/6-311+G*+ZPE)). The Na$_2$Cl value agrees with the experiment estimate (see Table II). The calculated adiabatic IPs of Li$_2$F (3.87 eV) and Na$_2$Cl (3.76 eV) are very close to the vertical electron affinities of corresponding cations calculated by the DV-X$_\alpha$ method (both 3.7 eV).[5b] The experimental IP of Na$_2$Cl, 4.15 ± 0.2 eV,[4b] is somewhat higher.

Li$_2$O, Na$_2$O, and Li$_2$S. A linear Li–O–Li geometry was deduced from molecular beam experiments.[22] The Li–O bond length of 1.60 ± 0.02 Å was obtained from gas-phase electron diffraction;[23] the vibrational frequencies, ν_2 = 112 cm^{-1} and ν_3 = 945.6 cm^{-1}, were determined by IR spectroscopy in matrix isolation.[24] HF

(16) Berkovitz, J.; Barson, C.; Goodman, G. *J. Chem. Phys.* **1980**, *77*, 631.

(17) Klimenko, N. M.; Zakzhevskii, V. G.; Charkin, O. P. *Koord. Khim.* **1982**, *8*, 903.

(18) Huber, K. P.; Herzberg, G. *Constants of Diatomic Molecules*; Van Nostrand Reinhold: New York, 1979.

(19) Thompson, J. W.; Child, M. S. *Chem. Phys. Lett.* **1989**, *157*, 343.

(20) Roach, A. C.; Child, M. S. *Mol. Phys.* **1968**, *14*, 1.

(21) Kappes, M.; Radi, P.; Schor, M.; Schumacher, E. *Chem. Phys. Lett.* **1985**, *113*, 243.

(22) Buchler, A.; Stauffer, J. L.; Klemperer, W. *J. Chem. Phys.* **1963**, *39*, 2299.

(23) Tolmachev, S. M.; Zasorin, E. Z.; Rambidi, N. G. *Zh. Strukt. Khim.* **1969**, *10*, 541.

(24) (a) Seshadri, K. S.; White, D.; Mann, D. E. *J. Chem. Phys.* **1966**, *45*, 4697. (b) Spiker, R. C.; Andrews, L. *J. Chem. Phys.* **1973**, *58*, 702.

Table I. Correlated Total Energies (–au)

species	MP2 (FULL)[a] 6-31+G*	ZPE[b]	PMP2(FC)[c] 6-31+G*, 6-311+G*, 6-311+G(2df)	PMP3(FC)[c] 6-31+G*, 6-311+G*, 6-311+G(2df)	PMP4(FC)[c] 6-31+G*, 6-311+G*, 6-311+G(2df)	QCISD[c] 6-31+G*, 6-311+G*, 6-311+G(2df)	QCISD(T)[c] 6-31+G*, 6-311+G*, 6-311+G(2df)	QCISD(T)[c]+ZPE[d] 6-31+G*, 6-311+G*, 6-311+G(2df)
Li+ (^{1}S)	7.235 99		7.235 54[e]					
			7.235 84[e]					
			7.235 84[e]					
Li (^{2}S)	7.432 11		7.431 56[e]					
			7.432 03[e]					
			7.432 03[e]					
Na+ (^{1}S)	161.660 87		161.659 29[e]					
			161.664 29[e]					
			161.664 29[e]					
Na (^{2}S)	161.843 74		161.841 44[e]					
			161.845 98[e]					
			161.845 98[e]					
Li$_2$ ($D_{\infty h}$, $^1\Sigma_g^+$)	14.887 48 (0)	0.5	14.885 97	14.892 13	14.894 81	14.897 01	14.897 01	14.896 26
			14.889 04	14.895 12	14.897 82	14.900 10	14.900 10	14.899 35
			14.891 08	14.896 64	14.899 24	14.901 59	14.901 59	14.900 84
Na$_2$ ($D_{\infty h}$, $^1\Sigma_g^+$)	323.704 27 (0)	0.2	323.698 67	323.703 68	323.705 78	323.707 37	323.707 37	323.707 07
			323.707 98	323.712 91	323.715 06	323.716 67	323.716 67	323.716 37
			323.710 09	323.714 53	323.716 59	323.718 28	323.718 28	323.717 98
LiF ($^1\Sigma_g^+$)	107.151 35 (0)	1.3	107.145 13	107.138 06	107.151 01	107.145 46	107.147 64	107.145 69
			107.205 18	107.196 21	107.210 82	107.203 63	107.208 10	107.206 15
			107.254 43	107.247 57	107.262 66	107.252 72	107.259 53	107.257 58
NaCl ($^1\Sigma_g^+$)	621.551 59 (0)	0.5	621.538 82	621.550 48	621.553 87	621.551 38	621.554 40	621.553 65
			621.577 14	621.588 35	621.592 18	621.589 30	621.592 65	621.591 90
			621.632 57	621.649 87	621.656 43	621.648 62	621.656 52	621.655 77
Li$_2$F+ ($D_{\infty h}$, $^1\Sigma_g^+$)	114.498 43 (0)	2.5	114.487 85	114.483 16	114.493 32	114.488 92	114.491 07	114.487 32
			114.549 65	114.543 19	114.554 93	114.549 03	114.553 11	114.549 36
			114.598 47	114.593 97	114.606 55	114.597 84	114.604 32	114.600 57
Li$_2$F (C_{2v}, ^{2}A$_1$)	114.638 55 (0)	2.3	114.629 07	114.624 22	114.635 56	114.630 80	114.633 40	114.629 95
			114.691 04	114.684 41	114.697 44	114.691 01	114.695 73	114.692 28
			114.740 78	114.736 16	114.749 92	114.740 66	114.747 81	114.744 36
Na$_2$Cl+ ($D_{\infty h}$, $^1\Sigma_g^+$)	783.291 34 (0)	1.0	783.274 76	783.286 80	783.289 77	783.287 37	783.290 19	783.288 69
			783.317 86	783.329 49	783.332 89	783.330 13	783.333 26	783.331 76
			783.372 55	783.390 25	783.396 64	783.388 88	783.396 73	783.395 23
Na$_2$Cl (C_{2v}, ^{2}A$_1$)	783.427 94 (0)	0.9	783.411 72	783.423 95	783.427 53	783.424 85	783.428 30	783.426 95
			783.454 14	783.465 90	783.469 91	783.466 85	783.470 63	783.469 28
			783.509 47	783.527 18		783.526 03	783.534 54	783.533 19
Li$_2$O ($D_{\infty h}$, $^1\Sigma_g^+$)	90.021 94 (2)	2.6	90.008 24	89.991 24	90.016 63	90.004 33	90.009 11	90.005 22
			90.048 49	90.028 54		90.042 75	90.050 64	90.046 75
			90.094 37	90.076 13	90.105 95	90.086 33	90.097 61	90.093 72
Li$_2$O (C_{2v}, ^{1}A$_1$)	90.021 96 (0)	2.7	90.008 17	89.991 14	90.016 64	90.004 29	90.009 07	90.005 03
			90.048 40	90.028 41	90.058 25	90.042 66	90.050 57	90.046 53
			90.094 24	90.075 96	90.105 88	90.086 20	90.097 50	90.093 46
Li$_3$O+ (D_{3h}, ^{1}A$_1'$)	97.401 67 (0)	4.7	97.382 08	97.371 49	97.389 38	97.380 55	97.385 19	97.377 70
			97.423 80	97.410 28	97.432 20	97.420 34	97.427 72	97.420 23
			97.467 90	97.456 18	97.478 32	97.463 12	97.473 29	97.465 80
Li$_3$O (D_{3h}, ^{2}A$_1'$)	97.529 62 (0)	4.2	97.509 50	97.498 45	97.519 74	97.509 53	97.515 82	97.509 53
			97.551 11	97.537 30	97.562 42	97.549 22	97.558 42	97.551 73
			97.595 76	97.583 62		97.592 04	97.604 18	97.597 89
Li$_4$O^{2+} (T_d, ^{1}A$_1$)	104.589 80 (0)	5.8	104.565 48	104.557 07	104.572 31	104.564 66	104.569 19	104.560 50
			104.607 07	104.596 54	104.615 87	104.605 20	104.612 33	104.603 64
			f					
Na$_2$O ($D_{\infty h}$, $^1\Sigma_g^+$)	398.759 53 (0)	1.5	398.746 78	398.715 19	398.765 98	398.745 77	398.739 62	398.737 23
			398.789 69	398.754 85	398.810 50	398.785 59	398.787 23	398.784 84
			398.836 32	398.803 37	398.857 06	398.825 36	398.835 58	398.833 33
Na$_3$O+ (D_{3h}, ^{1}A$_1'$)	560.544 27 (0)	2.6	560.523 71	560.504 13	560.533 96	560.519 36	560.524 25	560.520 11
			560.572 45	560.549 89	560.584 09	560.566 20	560.574 25	560.570 36
			560.618 35	560.597 69	560.631 11	560.609 52	560.620 89	560.617 00
Na$_3$O (D_{3h}, ^{2}A$_1'$)	560.662 43 (0)	2.5	560.643 20	560.620 22	560.659 08	560.640 47	560.646 79	560.642 81
			560.691 57	560.665 60	560.708 87	560.686 72	560.696 80	560.692 82
			560.736 59	560.712 46	560.754 51	560.728 87	560.742 80[g]	560.739 05[g]
Li$_2$S (C_{2v}, ^{1}A$_1$)	412.639 23 (0)	1.9	412.625 17	412.636 32	412.643 11	412.634 08	412.643 96	412.640 93
			412.663 59	412.674 39	412.682 07	412.675 88	412.682 76	412.679 73
			412.710 48	412.726 06	412.735 67	412.724 42	412.735 51	412.732 48
Li$_2$S ($D_{\infty h}$, $^1\Sigma_g^+$)	412.638 56 (0)	2.2	412.623 36	412.634 82	412.640 88	412.636 37	412.641 70	412.638 19
			412.660 76	412.671 83	412.678 80	412.673 33	412.679 50	412.675 99
			412.710 26	412.726 04	412.735 05	412.724 31	412.734 90	412.731 39
Li$_3$S+ (D_{3h}, ^{1}A$_1'$)	419.994 84 (0)	1.8	419.979 05	419.991 26	419.996 29	419.991 83	419.996 87	419.994 00
			420.018 45	420.030 45	420.036 29	420.030 92	420.036 78	420.033 91
			420.064 45	420.081 22	420.089 59	420.079 31	420.089 50	420.086 90
Li$_3$S (C_{3v}, ^{2}A$_1$)	420.125 35 (0)	2.8	420.108 90	420.121 32	420.128 47	420.123 08	420.130 17	420.125 71
			420.149 21	420.161 37	420.169 38	420.162 90	420.170 94	420.166 48
			420.195 12	420.211 75	420.222 07			
Li$_3$S (C_{2v}, ^{2}A$_1$)	420.121 24 (1)	2.6	420.105 23	420.117 68	420.123 81	420.119 19	420.125 22	420.121 08
Li$_3$N (D_{3h}, ^{1}A$_1'$)	76.996 37 (0)	4.4	76.977 98	76.951 28	76.995 99	76.972 77	76.982 98	76.975 97
			77.006 49	76.978 36	77.025 76	76.999 33	77.012 30	77.005 29
			77.042 63	77.015 20		77.031 23	77.048 16	77.041 57

Table I. (Continued)

species	MP2 (FULL)[a] 6-31+G*	ZPE[b]	PMP2(FC)[c] 6-31+G*, 6-311+G*, 6-311+G(2df)	PMP3(FC)[c] 6-31+G*, 6-311+G*, 6-311+G(2df)	PMP4(FC)[c] 6-31+G*, 6-311+G*, 6-311+G(2df)	QCISD[c] 6-31+G*, 6-311+G*, 6-311+G(2df)	QCISD(T)[c] 6-31+G*, 6-311+G*, 6-311+G(2df)	QCISD(T)[c]+ZPE[d] 6-31+G*, 6-311+G*, 6-311+G(2df)
Li_3P (C_{3v}, $^1A_1$)	363.250 64 (0)	3.0	363.233 44	363.243 88	363.256 03	363.246 26	363.256 90	363.252 12
			363.267 49	363.277 69	363.290 60	363.279 47	363.291 11	363.286 33
			363.304 81	363.317 72	363.332 04	363.315 81	363.331 35	363.326 86
Li_3P (D_{3h}, $^1A_1'$)	363.240 73 (1)	1.7						
Li_4N^+ (T_d, $^1A_1$)	84.384 24 (0)	6.2	363.259 76	363.270 46	363.281 18	363.271 40	363.281 61	363.278 90
			84.358 60	84.343 25	84.371 68	84.354 99	84.365 20	84.355 32
			84.388 42	84.371 52	*f*	84.383 32	84.395 64	84.385 76
Li_4N (T_d, $^2A_1$)	84.506 72 (0)	5.7[h]	84.485 65	84.472 36	84.501 80	84.483 35	84.496 47	84.487 93
			84.515 33	84.500 61	84.532 80	84.511 64	84.526 91	84.518 37
			f					
Li_4P^+ (T_d, $^1A_1$)	370.613 45 (0)	3.7	370.594 50	370.606 95	370.614 69	370.607 16	370.615 29	370.609 39
			370.631 77	370.644 20	370.652 74	370.644 04	370.653 15	370.647 25
			f					
Li_4P (C_{2v}, $^2A_1$)	370.736 71 (0)		370.716 84	370.728 58	370.739 61	370.729 60	370.741 26	
			370.753 16	370.764 70	370.776 63	370.765 33	370.778 04	
			f					

[a] Number of imaginary frequencies in parentheses. [b] Zero point energy. [c] MP2(FULL)/6-31+G* geometry. [d] Scaled by 0.94.[10] [e] Equivalent to HF values. [f] Exceeded our computational resources. [g] Estimated value. [h] MP2(FULL)/6-31G* geometry.

ab initio calculations with different basis sets also favored a linear $D_{\infty h}$ structure for Li_2O.[5a,c,25] Very extensive HF calculations with large STO basis sets gave an equilibrium bond length of 1.595 Å, which coincides with the experimental value. Similarly, linear Li–S–Li structures were calculated at HF/6-31G*[25c,g,26] with a Li–S bond length of 2.12 Å. However, our MP2(FULL)/6-31+G* geometry optimizations for both Li_2O and Li_2S led to lower energy angular C_{2v} configurations (see Figure 1b) with equilibrium bond lengths and valence angles of 1.635 Å/169.4° for Li_2O and 2.116 Å/114.9° for Li_2S. The linearization barriers are very small in both cases, and Li_2O and Li_2S in their ground states are "quasilinear" with large deformation amplitudes. Moreover, geometry optimization of Li_2S even at HF/6-31+G* led to an angular structure. Li_2O affords an additional example of a structure which changes preference from linear to bent when electron correlation corrections are included, e.g. at MP2(FULL) (see Table I). However, Na_2O is linear both at HF/6-31+G* and at MP2(FULL)/6-31+G* (the latter with Na–O = 2.029 Å; see Figure 1b).

As Li_2O and Li_2S are isoelectronic with H_2O, they are expected to have nonlinear structures. As shown by the NLMO analysis,[27] in the bent structures the lithium contributions to the hybrid overlap in the natural localized MOs prevail over the Coulomb repulsion of the positively charged Li atoms (which leads to a widening of the angle). This covalent contribution is manifest especially in SLi_2, but it is also significant enough in OLi_2 to influence the geometry.

The preference of linear or nonlinear structures of L_2O compounds (L = alkali metal atom) depends generally on the balance of covalent contributions to the L–O bond (which favors an angular structure) and of the repulsion between the positively charged ligands (which favors a linear structure). Correlation results in shifts of electron density in Li_2O and Li_2S from the doubly negatively charged central atom to the ligands. Since the bonds become more covalent, the structural preference of Li_2O changes to C_{2v}. With Na_2O, this correlation effect is not sufficient to overcome the repulsion between the Na^+ cations.

Li_3O^+, Li_3O, Li_3S^+, Li_3S, Na_3O^+, and Na_3O. The Li_3O^+, Li_3S^+, and Na_3O^+ cations were studied at HF levels previously.[5a,j,m] The most stable D_{3h} configurations, with R(Li–O) = 1.70 Å,[5j] 1.67 Å,[5a] R(Li–S) = 2.23 Å,[5j] and R(Na–O) = 2.02 Å,[5m] as well as dissociation energies for $Li_3O^+ \rightarrow Li_2O + Li^+$ (86.6 kcal/mol) and $Li_3S^+ \rightarrow Li_2S + Li^+$ (72.6 kcal/mol) were deduced.[5j] The adiabatic ionization potential, $Na_3O \rightarrow Na_3O^+$, was estimated to be 2.92 eV.[5m]

Geometry optimization at MP2(FULL)/6-31+G* for Li_3O^+, Li_3S^+, and Na_3O^+ also led to planar D_{3h} structures (no imaginary frequencies). Our bond lengths and dissociation energies agree with the earlier HF data (see Figure 1c and Table IV) because the bonding is highly ionic and electron correlation is not important.

The extra electrons in the planar D_{3h} forms of the neutral molecules, Li_3O, Na_3O, and Li_3S, occupy valence $2a_1$ MOs. These MOs are antibonding with respect to interactions between central atom and ligands but are ligand–ligand bonding (Figure 2).[5c] Therefore, the geometries of the neutral species and cations might differ—as in the M_2X cases—to take advantage of ligand–ligand bonding. However, MP2(FULL)/6-31+G* optimization still favored planar triangular D_{3h} geometries for Li_3O and Na_3O but gave a triangular pyramidal C_{3v} structure for Li_3S (see Figure 1c). The optimized M–L bond lengths are nearly the same in the neutral and in the corresponding cationic species: 1.682 Å (Li_3O) vs 1.696 Å (Li_3O^+), 2.205 Å (Li_3S) vs 2.192 Å (Li_3S^+), and 2.057 Å (Na_3O) vs 2.038 Å (Na_3O^+) (all data at MP2(FULL)/6-31+G*). Li_3O and Na_3O as cationic and neutral molecules have the same geometries because the ligand–ligand distances 2.913 and 3.562 Å are close to the optimum values (see Li_2F and Na_2Cl, above). For Li_3S the Li···Li separation in the D_{3h} structure (3.797 Å) is too large. Therefore, pyramidization occurs; the Li···Li distance of 3.067 Å in the C_{3v} form of Li_3S is quite close to that in D_{3h} Li_3O.

Li_3N and Li_3P. There is no experimental information about the structures, stabilities, and vibrational frequencies of the Li_3N and Li_3P molecules. HF ab initio geometry optimizations are available for Li_3N[5c,j,l,28,29] and for Li_3P.[5j,26,30] Planar D_{3h} and pyramidal C_{3v} structures were found for Li_3N and Li_3P, respectively, with bond lengths of 1.735 Å for Li–N[28] and 4.186 Å for Li–P as well as a 110.7° bond angle for ∠Li–P–Li.[30] Our optimizations at the correlated MP2(FULL)/6-31+G* level also led to the same preferences, D_{3h} geometry for Li_3N and C_{3v} for Li_3P with R(Li–N) = 1.744 Å, R(Li–P) = 2.257 Å, and ∠Li–

(25) (a) Grow, D. T.; Pitzer, R. M. *J. Chem. Phys.* **1977**, *67*, 4019. (b) Blickensderfer, R. P.; Jordan, K. D. *Chem. Phys.* **1979**, *41*, 193. (c) Kao, J. *J. Mol. Struct.* **1979**, *56*, 147. (d) Marynick, D. S.; Dixon, D. A. *J. Phys. Chem.* **1983**, *87*, 3430. (e) Curtiss, L. A.; Blauder, M. *J. Electrochem. Soc.* **1984**, *131*, 2271. (f) Siddarth, P.; Gopinathan, M. S. *J. Am. Chem. Soc.* **1988**, *110*, 96. (g) Mebel, A. M.; Klimenko, N. M.; Charkin, O. P. *Zh. Strukt. Khim.* **1988**, *29*, 357.
(26) Marsden, C. J. *J. Chem. Soc., Chem. Commun.* **1989**, *89*, 1356.
(27) Reed, A. E.; Weinhold, F. *J. Chem. Phys.* **1985**, *83*, 1736.

(28) Würthwein, E.-U.; Sen, K. D.; Pople, J. A.; Schleyer, P. v. R. *Inorg. Chem.* **1983**, *22*, 496.
(29) Armstrong, D. R.; Perkins, P. G.; Walker, G. T. *Theochem.* **1985**, *23*, 189.
(30) Marynick, D. S. *Chem. Phys. Lett.* **1980**, *75*, 550.

Table II. Correlated Reaction Energies (kcal/mol) at MP2(FULL)/6-31+G* Geometries

reacn	MP2-FU 6-31+G*	MP2(FC) 6-31+G*, 6-311+G*, 6-311+G(2df)	MP3(FC) 6-31+G*, 6-311+G*, 6-311+G(2df)	MP4(FC) 6-31+G*, 6-311+G*, 6-311+G(2df)	QCISD(T) 6-31+G*, 6-311+G*, 6-311+G(2df)	QCISD(T)+ZPE[a] 6-31+G*, 6-311+G*, 6-311+G(2df)	exptl
1. Li$_2$ → 2Li	14.6	14.3	18.2	19.9	21.3	20.8	22.7[2j]
		15.7	19.5	21.2	22.6	22.1	23.7[38]
		17.0	20.4	22.1	23.5	23.1	25.5 ± 1.5[2b]
2. Na$_2$ → 2Na	10.5	9.9	13.1	14.4	15.4	15.2	16.9[39]
		10.1	13.1	14.5	15.5	15.3	17.0[38]
		11.4	14.2	15.5	16.5	16.3	
3. Li$_2$F$^+$ → LiF + Li$^+$	69.7	67.3	68.8	67.0	67.7	66.6	
		68.2	69.7	67.9	68.5	67.4	
		67.9	69.4	68.4	68.4	67.2	
4. Li$_2$F → LiF + Li	34.6	32.9	34.3	33.2	34.0	33.1	
		33.8	35.2	34.3	34.9	33.9	
		34.1	35.5	34.7	35.3	34.4	
5. Na$_2$Cl$^+$ → NaCl + Na$^+$	49.5	48.1	48.3	48.1	48.0	47.5	41.3[16]
		48.0	48.2	48.0	47.9	47.4	36.7[4b]
		47.5	47.7	47.6	47.6	47.2	
6. Na$_2$Cl → NaCl + Na	20.5	19.7	20.1	20.2	20.4	20.0	14.3[4b]
		19.5	19.8	19.9	20.1	19.7	18.0[21]
		19.4	19.7		20.1	19.7	
7. Li$_3$O$^+$ → Li$_2$O + Li$^+$	90.2	86.8	90.8	86.1	88.2	86.2	
		87.6	91.6	86.7	88.7	86.7	
		86.5	90.6	85.7	87.8	85.8	
8. Li$_4$O^{2+} → Li$_3$O$^+$ + Li$^+$	−30.0	−32.7	−31.3	−33.0	−32.3	−33.1	
		−33.0	−31.1	−32.7	−32.1	−32.9	
9. Li$_3$O → Li$_2$O + Li	47.4	43.7	47.5	44.9	47.1		50.7 ± 10.0[4a,40]
		44.3	48.2	45.3	47.6	46.1	
		43.6	47.5	44.5	46.8	45.6	
10. Na$_3$O$^+$ → Na$_2$O + Na$^+$	77.7	73.8	80.1	78.2	78.6	77.5	
		74.3	82.0	68.6	77.0	76.1	
11. Na$_3$O → Na$_2$O + Na	37.1	34.5	39.9	32.4	41.2	40.2	
		35.1	40.6	32.9	39.9	38.9	
		34.1	39.6	32.3			
12. Li$_4$N$^+$ → Li$_3$N + Li$^+$	95.3	91.0	98.2	87.8	92.0	90.2	
		91.7	98.7		92.6	90.8	
13. Li$_4$N → Li$_3$N + Li	49.1	48.4	56.8		51.4	50.4	
		48.2	56.6	47.1	51.8	50.9	
14. Li$_3$S$^+$ → Li$_2$S + Li$^+$	75.0	74.3	74.9	73.8	73.6	73.7	
		74.7	75.4	74.3	74.2	74.3	
		74.1	74.9	74.1	74.1	74.3	
15. Li$_3$S → Li$_2$S + Li	33.9	32.7	33.5	33.8	34.3	33.4	45.4 ± 10.3[6]
		33.6	34.5	34.7	35.2	34.3	
		33.1	33.7	34.2	34.7	33.9	
16. Li$_4$P$^+$ → Li$_3$P + Li$^+$	79.6	78.8	80.0	77.3	77.1	76.4	
		80.6	82.0	79.2	79.2	78.5	
17. Li$_4$P → Li$_3$P + Li	33.9	32.6	33.4	32.7	33.1		44.5 ● 5.7[4i]
		34.0	34.8	33.9	34.4		

[a] Scaled by 0.94.[10]

P–Li = 94.9° (Figure 1d). Our inversion barrier for Li$_3$P, 4.7 kcal/mol at QCISD(T)/6-311+G* + ZPE//MP2(FULL)/6-31+G*, is somewhat larger than the 2.2 kcal/mol CISD value.[30] Calculated frequencies (Table III) may help to identify these molecules in the gas phase or in matrix isolation.

Li$_4$N$^+$, Li$_4$N, Li$_4$P$^+$, and Li$_4$P. The Li$_4$P$^+$ cation was detected in mass spectrometric experiments,[4i] but experimental structures for Li$_4$N$^+$ and Li$_4$P$^+$ do not exist. Ab initio calculations assumed tetrahedral structures; equilibrium bond lengths were calculated at HF/3-21G (Li–N = 1.80 Å)[5c] and at HF/3-21G* (Li–N = 1.83 Å, Li–P = 2.32 Å).[5j] The calculated dissociation energies of Li$_4$N$^+$ → Li$_3$N + Li$^+$ and Li$_4$P$^+$ → Li$_3$P + Li$^+$ were 89.8 and 84.3 kcal/mol at MP3/DZP.[5k] We optimized the geometries of both cations at MP2(FULL)/6-31+G* in T_d symmetry and found them to be the global minima (no imaginary frequencies; see Table III). Our bond lengths 1.790 Å (Li$_4$N$^+$) and 2.275 Å (Li$_4$P$^+$) differ little from the previous ab initio data.[5c,j] The same is true for our calculated dissociation energies of 90.8 kcal/mol for Li$_4$N$^+$ and 78.5 kcal/mol for Li$_4$P$^+$ (QCISD(T)/6-311+G*+ZPE).

For the neutral Li$_4$P molecule the heat of formation and a dissociation energy into Li$_3$P + Li (44.5 kcal/mol) have been measured by high-temperature thermochemistry.[4i] Ab initio data are available for Li$_4$N[5c] but not for Li$_4$P. The valence electronic

configuration of both Li$_4$N$^+$ and Li$_4$P$^+$ is $(1a_1)^2(1t_2)^6(2a_1)^0$; therefore, the extra electron of the neutral Li$_4$N and Li$_4$P species should occupy the 2a$_1$ MO in T_d symmetry. This MO is antibonding with respect to central atom–ligand interactions but ligand–ligand bonding (see Figure 2c). According to our MP2-(FULL)/6-31+G* calculations, Li$_4$N favors tetrahedral symmetry with Li–N = 1.778 Å (Figure 1e). As in Li$_3$O and Na$_3$O, the neutral Li$_4$N and charged Li$_4$N$^+$ species prefer structures with the same symmetry because in neutral Li$_4$N the Li···Li distances (2.903 Å) are nearly optimum. Indeed, the bonding Li···Li interactions result in Li···Li distances even shorter in Li$_4$N than in Li$_4$N$^+$. However, the C_{2v} structure of Li$_4$P (see Figure 1e) differs from the T_d geometry favored by the corresponding Li$_4$P$^+$ cation. The explanation of the instability of the T_d structure for Li$_4$P is the same as discussed above for Li$_3$S. The Li···Li distances (3.669 Å) in T_d Li$_4$P are too large to permit optimum overlap between the Li AOs; therefore Li$_4$P distorts to C_{2v} symmetry. While one edge of the tetrahedron increases to 4.500 Å, the other Li···Li distances decrease to 3.338 Å (see Figure 1e). The last separation is closer to the Li···Li distance in Li$_3$O, Li$_3$S (C_{3v}), and Li$_4$N.

The same kind of distortion has been noted before in Li$_4$F.[5c] The closed shell system Li$_4$Si and Li$_4$S favor similar structures as well. The C_{2v} geometry of Li$_4$Si is 6.6 kcal/mol lower in energy

Table III. Adiabatic Ionization Potentials (eV) at MP2(FULL)/6-31+G* Geometries

reacn	MP2-FU 6-31+G*	MP2(FC) 6-31+G*, 6-311+G*, 6-311+G(2df)			MP3(FC) 6-31+G*, 6-311+G*, 6-311+G(2df)			MP4(FC) 6-31+G*, 6-311+G*, 6-311+G(2df)			QCISD(T) 6-31+G*, 6-311+G*, 6-311+G(2df)			QCISD(T)+ZPE[a]	exptl
1. Li → Li+	5.34	5.33			5.33			5.33			5.33				5.39[1]
		5.34			5.34			5.34			5.34				
		5.34			5.34			5.34			5.34				
2. Na → Na+	4.98	4.96			4.96			4.96			4.96				5.14[37]
		4.94			4.94			4.94			4.94				
		4.94			4.94			4.94			4.94				
3. Li2F → Li2F+	3.81	3.84			3.84			3.87			3.87			3.88	
		3.85			3.84			3.88			3.88			3.89	
		3.87			3.87			3.90			3.90			3.91	
4. Na2Cl → Na2Cl+	3.72	3.73			3.73			3.75			3.76			3.76	4.15 ± 0.2[4b]
		3.71			3.71			3.73			3.74			3.74	
		3.73			3.73						3.75			3.75	
5. Li3O → Li3O+	3.48	3.47			3.45			3.55							4.5 ● 0.2[4a]
		3.46			3.46			3.54			3.56			3.58	
		3.48			3.47			3.55			3.56			3.59	
6. Na3O → Na3O+	3.22	3.25			3.16			3.40			3.33			3.34	3.90 ± 0.1[2c]
		3.24			3.15			3.40			3.33			3.33	
		3.22			3.12			3.36							
7. Li4N → Li4N+	3.33	3.49			3.54						3.57			3.61	
		3.45			3.51						3.56			3.61	
8. Li3S → Li3S+	3.55	3.53			3.54			3.60			3.63			3.58	6.6 ± 0.2[6]
		3.56			3.56			3.62			3.65			3.61	
		3.56			3.55			3.61			3.63			3.58	
9. Li4P → Li4P+	3.35	3.27			3.31			3.40			3.43				
		3.30			3.28			3.37			3.40				

a Scaled by 0.94.[10]

than the T_d form (MP2/6-31G*//3-21G(*)).[31] A similar minimum exists for Li4S, although this is not the global minimum (E_{rel} = 8.26 kcal/mol at HF/6-31G*).[32]

The optimum ligand–ligand distances, ca. 2.9 Å for Li⋯Li and ca. 3.3 Å for Na⋯Na, may be useful to help interpret possible distortions of the neutral ML_{k+1} species with other central atoms from the structures of the corresponding ML_{k+1}^+ cations. These optimum ligand–ligand distances may also help to explain structural distortions from these expected in molecules where bonding ligand–ligand interactions are important. For example, the Li4O molecule is tetrahedral (with a Li⋯Li distance of 2.815 Å at HF/6-31G*), but the isoelectronic Li4S molecule prefers C_{3v} symmetry (S atom coordinated to a Li4 tetrahedron[32]). The ligand–ligand distances (3.634 Å) are too large in the T_d Li4S structure.

Low experimental IPs for the other superalkali systems, for KH2O (3.92 ± 0.04 eV), KNH3 (3.87 ± 0.04 eV), K2NH2 (3.94 ± 0.08 eV), and K2OH (3.55 ± 0.08 eV),[4e] are comparable to the IPs of the superalkalis studied here.

Bonding in Superalkalis. The stability of the cations (Li2F+, Na2Cl+, Li3O+, Li3S+, Na3O+, Li4N+, and Li4P+) is due to the electrostatic attraction of the Li+ or Na+ cations to the negative charged central atom (natural population and natural bond orbital analyses[33,34] are given in Figure 1a–e). The L–M bonds in all these cations are essentially fully ionic. On the basis of electrostatic repulsion of the cations' linear Li2F+ and Na2Cl+ $D_{∞h}$ structures, planar triangular D_{3h} structures for Li3O+, Li3S+, and Na3O+ and tetrahedral T_d structures for Li4N+ and Li4P+ can be expected.

According to classical theories of valence, the neutral superalkali species ML_{k+1} should not be stable, because the maximum "combining capacity" is one for F and Cl, two for O and S, and three for N and P; the central atom would have to "accept" more electrons and thus violate the octet rule. However, the bonding in neutral ML_{k+1} species is significantly different from such

classical models: while the central atoms possess nearly maximum anionic charges (F-, Cl-, O2-, S2-, N3-, and P3-), the lithium and sodium charges are less than the unit values (e.g. as found in ML_{k+1}^+ cations). The stability of neutral superalkali species is due both to the attractive electrostatic interactions between ligands and the central atom and in all superalkali ML_{k+1} molecules to the covalent interactions between ligands.

The HOMOs all have the same character, antibonding with respect to central atom–ligand interactions but ligand–ligand bonding (see Figure 2). The HOMOs are mainly comprised of the ligand AOs. The NH4 molecule is also stable (see ref 35 and references there), but the nature of the bonding differs fundamentally from that in Li4N. The HOMO of NH4 is a Rydberg nitrogen AO (essentially no contributions from the hydrogen AO). The corresponding antibonding MO in NH4 is higher than the Li4N HOMO. This change in the bonding character is due to the Li–Li interactions (the valence orbitals of alkali metals are more diffuse than the 1s AOs of hydrogen). Therefore, the antibonding MOs of the hyperlithiated compounds are lower in energy than the Rydberg AOs of the central atoms.

Speculations on Experimental Realization. While nearly all the permetalated cationic species we have discussed have been detected experimentally in the gas phase[4d,i,6,16] and the Li2F+ cation was found in molten [(K,Na),Li][F,NO3] salt systems with a total concentration relationship $C_{Li} > C_F$,[36] no solid salts containing superalkali cations have been recognized. We suggest that molecules like Li3O+Cl-, Li4N+Br-, etc. may be prepared in matrix isolation by condensing gas-phase mixtures of Li2O and LiCl, Li3N and LiBr, etc. Solid-state substances with superalkali cations might be prepared by melting Li2O and LiBF4, or similar pairs of salts, in 1:1 stoichiometric proportions. As mentioned above, the Li2F+ cation was detected in a molten mixture of salts. The calculated frequencies and IR intensities of superalkali cations (Table III) may help to identify these molecules e.g. in matrixes.

Moreover, multicharged cations like Li4O2+,[5a,c,37] Li6P2+, etc. may also be stable in the crystal fields of the solid state. Although

(31) (a) Schleyer, P. v. R.; Reed, A. E. *J. Am. Chem. Soc.* **1988**, *110*, 4453.
(b) Reed, A. E.; Schleyer, P. v. R.; Janoschek, R. *J. Am. Chem. Soc.* **1991**, *113*, 1885.
(32) Rehm, E.; Schleyer, P. v. R. Unpublished results.
(33) Reed, A. E.; Weinhold, F. *QCPE Bull.* **1985**, *5*, 141.
(34) Reed, A. E.; Weinhold, F. *Chem. Rev.* **1988**, *88*, 899.

(35) (a) Williams, B. W.; Porter, R. F. *J. Chem. Phys.* **1982**, *73*, 5598. (b) Gellene, G. I.; Cleary, D. A.; Porter, R. F. *J. Chem. Phys.* **1983**, *77*, 287.
(36) Bengtsson, L.; Holmberg, B.; Ulvenlund, S. *Inorg. Chem.* **1990**, *29*, 3615.
(37) Jug, K. *J. Comput. Chem.* **1984**, *5*, 555.

Table IV. Frequencies (cm^{-1}), Zero Point Energies (ZPE, in kcal/mol), and IR Intensities (in Parentheses, km/mol)

species, geometry	sym state	NIMAG[a]	freq	HF/6-31G*	MP2(FULL)/6-31+G*
Li$_2$O, $D_{\infty h}$	$^1\Sigma_g^+$	0/1	ν_1 (σ_g)	858 (0.0)	769
			ν_2 (σ_u)	1137 (454)	1027
			ν_3 (π_u)	133 (237)	46i
			ZPE[b]	3.2	2.6
Li$_2$O, C_{2v}	^{1}A$_1$	0/0	ν_1 (a$_1$)		774
			ν_2 (a$_1$)		64
			ν_3 (b$_2$)		1027
			ZPE[b]		2.7
Li$_3$O$^+$, D_{3h}	^{1}A$_1'$	0/0	ν_1 (a$_1'$)	727	685 (0.0)
			ν_2 (a$_2''$)	272	285 (288)
			ν_3 (e$'$)	874	843 (286)
			ν_4 (e$'$)	291	305 (75)
			ZPE[b]	4.8	4.7
Li$_3$O, D_{3h}	^{2}A$_1'$	0/0	ν_1 (a$_1'$)		699 (0.0)
			ν_2 (a$_2''$)		148 (0.0)
			ν_3 (e$'$)		859 (181)
			ν_4 (e$'$)		188 (592)
			ZPE[b]		4.2
Li$_4$O^{2+}, T_d	^{1}A$_1$	0/0	ν_1 (a$_1$)		557
			ν_2 (e)		266
			ν_3 (t$_2$)		627
			ν_4 (t$_2$)		365
			ZPE[b]		5.8
Li$_3$N, D_{3h}	^{1}A$_1'$	0/0	ν_1 (a$_1'$)	707 (0.0)	641
			ν_2 (a$_2''$)	144 (160)	202
			ν_3 (e$'$)	915 (254)	852
			ν_4 (e$'$)	236 (66)	257
			ZPE[b]	4.5	4.4
Li$_4$N$^+$, T_d	^{1}A$_1$	0/0	ν_1 (a$_1$)	643 (0.0)	606 (0.0)
			ν_2 (e)	237 (0.0)	264 (0.0)
			ν_3 (t$_2$)	776 (276)	760 (149)
			ν_4 (t$_2$)	312 (114)	303 (60)
			ZPE[b]	6.3	6.2
Li$_4$N$^+$, D_{4h}	^{1}A$_1$	1/-	ν_1 (a$_{1g}$)	479	
			ν_2 (a$_{2u}$)	58	
			ν_3 (b$_{1g}$)	466	
			ν_4 (b$_{2g}$)	303	
			ν_5 (b$_{2u}$)	20i	
			ν_6 (e$_u$)	648	
			ν_7 (e$_u$)	280	
			ZPE[b]	4.0	
Li$_4$N, T_d	^{2}A$_1$	0/0	ν_1 (a$_1$)	573 (0.0)	710 (0.0)[c]
			ν_2 (e)	192 (0.0)	225 (0.0)[c]
			ν_3 (t$_2$)	749 (1.0)	788 (404)[c]
			ν_4 (t$_2$)	193 (194)	149 (1229)[c]
			ZPE[b]	5.4	5.7[c]
Li$_4$N, D_{4h}	^{2}A$_{1g}$	1/-	ν_1 (a$_{1g}$)	530 (0.0)	
			ν_2 (a$_{2u}$)	227 (113)	
			ν_3 (b$_{1g}$)	493 (0.0)	
			ν_4 (b$_{2g}$)	275 (0.0)	
			ν_5 (b$_{2u}$)	169i (0.0)	
			ν_6 (e$_u$)	739 (2.9)	
			ν_7 (e$_u$)	204 (1974)	
			ZPE[b]	4.9	
Li$_4$N, C_{2v}	^{2}A$_1$	1/-	ν_1 (a$_1$)	872 (750)	
			ν_2 (a$_1$)	614 (22)	
			ν_3 (a$_1$)	282 (127)	
			ν_4 (a$_1$)	178 (13)	
			ν_5 (b$_1$)	111 (48)	
			ν_6 (b$_1$)	63 (61)	
			ν_7 (b$_2$)	661 (76)	
			ν_8 (b$_2$)	188 (7.4)	
			ν_9 (b$_2$)	169i (23)	
			ZPE[b]	4.2	
Li$_2$S, C_{2v}	^{1}A$_1$	0/0	ν_1 (a$_1$)		583
			ν_2 (a$_1$)		128
			ν_3 (b$_2$)		637
			ZPE[b]		1.9
Li$_2$S, $D_{\infty h}$	$^1\Sigma_g^+$	2/0	ν_1 (σ_g)		588
			ν_2 (σ_u)		658
			ν_3 (π_u)		127
			ZPE[b]		2.1
Li$_3$S$^+$, D_{3h}	^{1}A$_1'$	0/0	ν_1 (a$_1'$)		482
			ν_2 (a$_2''$)		102
			ν_3 (e$'$)		547
			ν_4 (e$'$)		140
			ZPE[b]		1.8
Li$_3$S, C_{3v}	^{2}A$_1$	0/0	ν_1 (a$_1$)		546 (31)
			ν_2 (a$_1$)		144 (18)
			ν_3 (e)		507 (3.1)
			ν_4 (e)		119 (210)
			ZPE[b]		2.8

species, geometry	sym state	NIMAG[a]	freq	HF/6-31G*	MP2(FULL)/6-31+G*
Li$_3$S, C_{2v}	^{2}A$_1$	1/-	ν_1 (a1)	618 (240)	
			ν_2 (a$_1$)	495 (16)	
			ν_3 (a$_1$)	260 (23)	
			ν_1 (b$_1$)	23i (44)	
			ν_5 (b$_2$)	426 (16)	
			ν_6 (b$_2$)	67 (32)	
			ZPE[b]	2.7	
Li$_3$P, C_{3v}	^{1}A$_1$	0/0	ν_1 (a$_1$)		503 (1.3)
			ν_2 (a$_1$)		172 (46)
			ν_3 (e)		532 (64)
			ν_4 (e)		169 (5.2)
			ZPE[b]		3.0
Li$_3$P, D_{3h}	^{1}A$_1$	1/3	ν_1 (a$_8'$)		500
			ν_2 (a$_2''$)		80i
			ν_3 (e$'$)		362
			ν_4 (e$'$)		357i
			ZPE[b]		1.7
Li$_4$P$^+$, T_d	^{1}A$_1$	0/0	ν_1 (a$_1$)	457 (0.0)	445 (0.0)
			ν_2 (e)	133 (0.0)	141 (0.0)
			ν_3 (t$_2$)	510 (182)	517 (153)
			ν_4 (t$_2$)	129 (82)	106 (60)
			ZPE[b]	3.8	3.5
Li$_4$P$^+$, D_{4h}	^{1}A$_{1g}$	1/-	ν_1 (a$_{1g}$)	472 (0.0)	
			ν_2 (a$_{2u}$)	94 (164)	
			ν_3 (b$_{1g}$)	446 (0.0)	
			ν_4 (b$_{2g}$)	261 (0.0)	
			ν_5 (b$_{2u}$)	106i (0.0)	
			ν_6 (e$_u$)	527 (312)	
			ν_4 (e$_u$)	189 (30)	
			ZPE[b]		
Li$_4$P, C_{3v}	^{2}A$_1$	0/-	ν_1 (a$_1$)	574 (125)	
			ν_2 (a$_1$)	470 (1.2)	
			ν_3 (a$_1$)	168 (3.8)	
			ν_4 (e)	457 (0.9)	
			ν_5 (e)	109 (243)	
			ν_6 (e)	52 (43)	
			ZPE[b]	3.5	
Li$_4$P, T_d	^{2}A$_1$	3/-	ν_1 (a$_1$)	449 (0.0)	
			ν_2 (e)	54 (0.0)	
			ν_3 (t$_2$)	484 (626)	
			ν_4 (t$_2$)	103i (391)	
			ZPE$_b$	2.9	
Li$_4$P, C_{2v} (I)	^{2}A$_1$	0/0	ν_1 (a$_1$)	498 (11)	
			ν_2 (a$_1$)	459 (12)	
			ν_3 (a$_1$)	143 (17)	
			ν_4 (a$_1$)	93 (12)	
			ν_5 (a$_2$)	142 (0.0)	
			ν_6 (b$_1$)	510 (419)	
			ν_7 (b$_2$)	120 (48)	
			ν_8 (b$_2$)	527 (18)	
			ν_9 (b$_2$)	150 (232)	
			ZPE[b]	3.8	
Li$_4$P, C_{2v} (II)[d]	^{2}A$_1$	0/-	ν_1 (a$_1$)	524 (47)	
			ν_2 (a$_1$)	457 (13)	
			ν_3 (a$_1$)	222 (0.1)	
			ν_4 (a$_1$)	82 (67)	
			ν_5 (a$_2$)	100 (0.0)	
			ν_6 (b$_1$)	565	
			ν_7 (b$_2$)	45 (8.6)	
			ν_8 (b$_2$)	404 (29)	
			ν_9 (b$_2$)	52 (31)	
			ZPE[b]	3.5	
Li$_4$P, D_{4h}	^{2}B$_{2g}$	1/-	ν_1 (a$_{1g}$)	478 (0.0)	
			ν_2 (a$_{2u}$)	34i (54)	
			ν_3 (b$_{1g}$)	473 (0.0)	
			ν_4 (b$_{2g}$)	310 (0.0)	
			ν_5 (b$_{2u}$)	32 (0.0)	
			ν_6 (e$_u$)	674 (7992)	
			ν_7 (e$_u$)	300 (1254)	
			ZPE[b]	4.6	
Na$_2$Cl$^+$, $D_{\infty h}$	$^1\Sigma_g^+$	0/-	ν_1 (σ_g)	222 (0.0)	
			ν_2 (σ_u)	321 (109)	
			ν_3 (π_u)	52 (71)	
			ZPE[b]	0.9	
Na$_3$O$^+$, D_{3h}	^{1}A$_1$	0/0	ν_1 (a$_1'$)		307 (0.0)
			ν_2 (a$_2''$)		203 (151)
			ν_3 (e$'$)		520 (132)
			ν_4 (e$'$)		147 (15)
			ZPE[b]		2.6
Na$_3$O, D_{3h}	^{2}A$_1$	0/0	ν_1 (a$_1'$)		316 (0.0)
			ν_2 (a$_2''$)		138 (4.3)
			ν_3 (e)		524 (24)
			ν_4 (e)		109 (31)
			ZPE[b]		2.5

[a] Number of imaginary frequencies at HF/MP2. [b] Unscaled. [c] MP2(FULL)/6-31G*. [d] This local minimum represents a variant of structure I (see Figure Ie), with a shortened Li$_{eq}$Li$_{eq}$ bond, an elongated PLi$_{eq}$ bond, and a decreased La$_{ax}$PLi$_{ax}$ angle.

having metastable minima in isolation (see Table IV), these doubly charged species are thermodynamically unstable and are likely to split off Li^+ (see Table II). The electrostatic repulsions between the ligands are high.

Conclusions

1. All the superalkalis we have investigated (Li_2F, Na_2Cl, Li_3O, Li_3S, Na_3O, Li_4N, and Li_4P) are thermodynamically stable toward loss of an alkali metal atom. All possess very low IPs—lower than the IP of the Cs atom, the lowest IP among the alkali metals. The low first ionization potentials in the superalkali species are due to the antibonding character of central atom–ligand bonding and to the electrostatic stabilization of the corresponding cations.

2. The structures of the superalkali species are determined mainly by the ligand–ligand bonding interactions in the HOMO of these species. The Li_3O, Na_3O, and Li_4N molecules possess the same high-symmetry geometries as the corresponding cations, Li_3O^+, Na_3O^+, and Li_4N^+. In contrast, the neutral Li_2F, Na_2Cl, Li_3S, and Li_4P prefer lower symmetry than their cations. These changes in geometrical preference result from the energy gain when optimum ligand–ligand distances (2.9 Å for Li⋯Li and 3.3 Å for Na⋯Na) are achieved. While the metal–metal distances are nearly optimum in the D_{3h} structures of Li_3O and Na_3O, lower symmetries are adopted by Li_2F and Na_2Cl (C_{2v} and not $D_{\infty h}$), Li_3S (C_{3v} and not D_{3h}), and Li_4P (C_{2v} and not T_d) in order to optimize the bonding ligand–ligand interactions.

(38) Huber, K. P.; Herzberg, G. *Molecular Spectra and Molecular Structure*; Van Nestrand Reinhold: New York, 1979.
(39) Wagman, D. D.; Evans, W. H.; Parker, V. B.; Schumm, R. H.; Halow, I.; Bailey, S. M.; Churney, K. L.; Nuttall, R. L. The NBS Tables of Chemical Thermodynamics Properties. *J. Phys. Chem. Ref. Data* **1982**, *11*, Suppl. 2.
(40) Kimura, H.; Asano, M.; Kubo, K. *J. Nucl. Mater.* **1980**, *92*, 221.